Anal. Chem. **1999,** *71,* 5297−5303

Simultaneous Determination of the $^2H/^1H$, $^{17}O/^{16}O$, and $^{18}O/^{16}O$ Isotope Abundance Ratios in Water by Means of Laser Spectrometry

E. R. Th. Kerstel,* R. van Trigt, N. Dam,† J. Reuss,† and H. A. J. Meijer

Centrum voor IsotopenOnderzoek, University of Groningen, Nijenborgh 4, Groningen, 9747 AG, The Netherlands

We demonstrate the first successful application of infrared laser spectrometry to the accurate, simultaneous determination of the relative $^2H/^1H$, $^{17}O/^{16}O$, and $^{18}O/^{16}O$ isotope abundance ratios in water. The method uses a narrow line width color center laser to record the direct absorption spectrum of low-pressure gas-phase water samples (presently 10 μL of liquid) in the 3-μm spectral region. It thus avoids the laborious chemical preparations of the sample that are required in the case of the conventional isotope ratio mass spectrometer measurement. The precision of the spectroscopic technique is shown to be 0.7‰ for δ^2H and 0.5‰ for $\delta^{17}O$ and $\delta^{18}O$ (δ represents the relative deviation of a sample's isotope abundance ratio with respect to that of a calibration material), while the calibrated accuracy amounts to about 3 and 1‰, respectively, for water with an isotopic composition in the range of the Standard Light Antarctic Precipitation and Vienna Standard Mean Ocean Water international standards.

Quantitative information on the natural variation of isotope abundance ratios is extremely useful, in fact often indispensable, information for a wide variety of research fields. For example, the $^{13}C/^{12}C$ ratio in CH_4 puts important constraints on the relative contributions to the global methane budget of the various CH_4 sources and their isotopic behavior.[1−3] Similarly, the data recorded on a global scale of the $^{13}C/^{12}C$ ratio in atmospheric CO_2 represent crucial independent information, which help to elucidate the role the oceans and the terrestrial biosphere have in the global carbon cycle, by virtue of the different rates of uptake of the two isotopic species.[4−7] The same $^{13}C/^{12}C$ isotope ratio in the CO_2 fraction of exhaled air for breath analysis is a valuable medical diagnostic tool, e.g., for the detection of *Heliobacter pylori* infections by means of a ^{13}C-labeled urea test or the quantification of the amino acid metabolism by means of a ^{13}C-labeled leucine test.[8]

But arguably it is the study of the isotopic composition of water that finds application in the widest variety of disciplines, from paleoclimatology to hydrology, atmospheric chemistry, and biomedicine.

For the field of paleoclimatology, both the ^{18}O and the ^2H isotopic composition depth profiles of ice cores recovered from polar ice sheets have proven to be among the most reliable and detailed proxy temperature records of the earth's past climate (dating back some 250 000 yr).[9−13] In addition, the interrelation of the ^{18}O and the ^2H abundances is sensitive to parameters other than the local temperature at the time of the polar precipitation, such as relative humidity and temperature in the source region. Knowledge of both isotope abundances thus provides important additional information.[14] For example, rapid climate changes during the last glacial period were identified by the combined $^{18}O-^2H$ analysis of a small section of the Greenland "DYE 3" ice core.[15] However, currently a complete analysis of such an ice core (with a total length of up to 3 km) is still prohibitively time-consuming.

Isotopic analysis of water is also an important tool in the hydrological study of groundwater and surface water systems. The ^{18}O and the ^2H isotopic signatures are indicative of the climatic conditions under which recharge took place and can be used to estimate retention times.

An example of a widespread application in biomedicine is the so-called doubly labeled water method for the quantification of

* Corresponding author: (fax) +31-50-363 4738; (e-mail) kerstel@phys.rug.nl.
† Molecular and Laser Physics, University of Nijmegen, The Netherlands.

(1) Stevens, C. M.; Engelkemeir, A. *J. Geophys. Res.* **1988**, *93*, 725−733.
(2) Schupp, M.; Bergamaschi, P.; Harris, G. W.; Crutzen, P. J. *Chemosphere* **1993**, *26*, 13−22.
(3) Bergamaschi, P.; Schupp, M.; Harris, G. W. *Appl. Opt.* **1994**, *33*, 7704−7716.
(4) Mook, W. G.; Koopmans, M.; Carter, A. F.; Keeling, C. D. *J. Geophys. Res.* **1983**, *88*, 10915−10933.
(5) Keeling, C. D.; Whorf, T. P.; Wahlen, M.; van der Plicht, J. *Nature* **1995**, *375*, 666−670.
(6) Ciais, P.; Tans, P. P.; White, J. W. C.; Trolier, M.; Francey, R. J.; Berry, J. A.; Randall, D. R.; Sellers, P. J.; Collatz, J. G.; Schimel, D. S. *J. Geophys. Res.* **1995**, *100*, 5051−5070.
(7) Francey, R. J.; Tans, P. P.; Allison, C. E.; Enting, I. G.; White, J. W. C.; Trolier, M. *Nature* **1995**, *373*, 326−330.
(8) Koletzko, S.; Haisch, M.; Seeboth, I.; Braden, B.; Hengels, K.; Koletzko, B.; Hering, P. *Lancet* **1995**, *345*, 961−962 and references therein. Murnick, D. E.; Colgan, M. J.; Lie, H. P.; Stoneback, D. *SPIE Proc.* **1996**, *2678*, 454−463.
(9) Petit, J. R.; Basile, I.; Raynaud, D.; Lorius, C.; Jouzel, J.; Stievenard, M.; Lipenkov, V. Y.; Barkov, N. I.; Kudryashov, B. B.; Davis, M.; Saltzman, E.; Kotlyakov, V. *Nature* **1997**, *387*, 359−359.
(10) Grootes, P. M.; Stuiver, M.; White, J. W. C.; Johnsen, S.; Jouzel, J. *Nature* **1993**, *366*, 552−554.
(11) Petit, J. R.; White, J. W. C.; Young, N. W.; Jouzel, J.; Korotkevich, S. *J. Geophys. Res.* **1991**, *96*, 5113−5122.
(12) Salamatin, A. N.; Lipenkow, V. Y.; Barkov, N. I.; Jouzel, J.; Petit J. R.; Raynaud, D. *J. Geophys. Res.* **1998**, *103*, 8963−8977.
(13) Johnsen, S. J.; Dahl-Jensen, D.; Dansgaard, W.; Gundestrup, N. *Tellus* **1995**, *47B*, 624−630.
(14) Armengaud, A.; Koster, R. D.; Jouzel J.; Ciais, P. *J. Geophys. Res.* **1998**, *103*, 8947−8953.
(15) Dansgaard, W.; White, J. W. C.; Johnsen, S. J. *Nature* **1989**, *339*, 532−534.

10.1021/ac990621e CCC: $18.00
Published on Web 10/28/1999

the metabolism of free-roaming animals in their natural habitat.[16] Here, water enriched in ^2H and ^{18}O is administered and the subsequent decrease in ^2H (due to loss of water) and ^{18}O (due to loss of water and CO_2) content of the body water pool is measured (typically after 24 h). From this, the CO_2 production can be calculated and, therewith, the energy expenditure.

At the same time, however, the currently available methods for the measurement of isotope ratios in water are far more cumbersome (as well as inaccurate) than for, for example, CO_2. Traditionally, all methods make use of isotope ratio mass spectrometers (IRMS) designed specifically for the purpose of measuring isotope abundance ratios. Due to the nature of the molecule, the water samples are not introduced directly into the mass spectrometer. Instead, the water is chemically converted to CO_2 and H_2, and the $^{18}O/^{16}O$ and $^2H/^1H$ isotope ratios are measured on the respective molecules. The conventional method for $^{18}O/^{16}O$ is to bring the water sample into contact with CO_2 of known isotopic composition and to wait several hours for the bicarbonate reaction to establish isotopic equilibrium (up to 24 h in the case of the original static equilibrium method, often referred to as the Epstein−Mayeda technique[17]). The H_2 is most commonly produced by reduction of water over hot (∼800 °C) uranium or zinc. These sample pretreatments are sometimes hazardous and almost always time-consuming, as well as the limiting factor in achieving the high accuracy demanded in the majority of studies. An additional disadvantage of the traditional IRMS method is the virtual impossibility of measuring the $^{17}O/^{16}O$ ratio in water, due to the mass overlap of $^{17}O^{12}C^{16}O$ and the much more abundant $^{16}O^{13}C^{16}O$.

It is in this light that there is much interest in alternative methods. The use of platinum catalytic equilibration of a water sample and hydrogen and/or carbon dioxide gas in combination with an IRMS appears promising.[18,19] But this method too has its disadvantages: the equilibrium state is accompanied by a very large isotope fractionation (about −740‰ at room temperature), which is also extremely temperature dependent (∼6‰/°C). Furthermore, the gas sample arriving at the IRMS contains approximately one-quarter the original amount of deuterium, considerably decreasing the (already low) mass-3 signal, with obvious consequences for errors due to background correction, amplifier offset, and, above all, the H_3^+ correction. Finally, the amount of water required is rather large (typically 4−5 mL), prohibiting the use of this method in quite a number of possible applications. The latter is also true for electrolysis.[20] In fact, the only realistic alternative appears to be on-line pyrolysis of water in combination with a continuous-flow IRMS. The latter method is able to deal with very small sample sizes (down to 1 μL), provides a high throughput, and is able to achieve very reasonable precisions (2‰ for δ^2H and ∼0.3‰ for $\delta^{18}O$; unfortunately the data presented by Begley and Scrimgeour are insufficient to give an estimate of the overall accuracy).[21]

Here we report on our efforts to use a completely different measurement technique, based on direct absorption laser spectroscopy. For most relatively small molecules the room-temperature, low-pressure gas-phase infrared spectra reveal absorptions due to individual rovibrational transitions that can each be uniquely assigned to one of the various isotopic species present. The absorption intensities of these lines, relative to that of a line belonging to the most abundant isotopic species, can be used to calculate the isotope ratio of interest. The measurement of the absorption intensity is done by recording the attenuation of a laser beam with narrow spectral line width as a function of its wavelength.

This technique has some major advantages over the traditional IRMS method: smaller sample sizes and direct measurement of isotope ratios in the water vapor, avoiding the time-consuming and inaccurate sample preparations that are otherwise required. Moreover, with the spectroscopic method, it is possible to accurately measure the $^{17}O/^{16}O$ ratio in water (in addition to the $^{18}O/^{16}O$ and $^2H/^1H$ ratios) as well as site-selective isotope ratios in more complex molecules. Both of these are impossible or completely impractical with the conventional mass spectrometer (including pyrolysis and continuous-flow systems) and provide ample opportunities for completely new research.

Spectroscopic methods have been applied previously to measure isotope ratios in other environmentally interesting molecules.[22,23] However, in most of the cases the accuracy obtained was not sufficient to make the instrument truly useful. In our opinion, so far the only successful application of laser spectroscopy has been the determination of the relative $^{13}C/^{12}C$ and $^2H/^1H$ ratios in methane, using a lead salt tunable diode laser system, in a careful study reported by Bergamaschi and co-workers.[2,3] They obtained precisions of, respectively, 0.5 and 3‰, while the overall accuracies were limited to 0.6 and 5‰.[3] Also, the nonlaser optical method of nondispersive infrared (NDIR) has shown its usefulness in the analysis of breath for the $^{13}C/^{12}C$ isotope ratio in CO_2.[8] Fusch and co-workers have applied Fourier transform infrared spectroscopy to the measurement of $^2H/^1H$ ratios in liquid water samples with a precision of ∼5‰ at low deuterium enrichment levels.[24] Unfortunately, as the method relies on the large change in vibrational frequency associated with the OH bond upon ^2H substitution in order to achieve isotope specificity, it cannot be used to measure the oxygen isotope ratio(s). This, together with the somewhat low accuracy, effectively restricts their method to applications in the field of biomedicine.

In this paper, we report what to the best of our knowledge is the first successful application of laser spectroscopy to the accurate determination of isotope abundance ratios in water.

EXPERIMENTAL SECTION

The apparatus, depicted in Figure 1, uses as its light source a tunable near-infrared, single-mode, color center laser (Burleigh FCL-20). It produces ∼14 mW at 2.7 μm into a 3-MHz line width, when pumped with 0.7 W of a krypton ion laser (at 647 nm). The reliability of the laser system is determined almost entirely by the lifetime of the pump laser. The current laser has been

(16) Prentice, A. M., Ed. *The Doubly-Labeled Water Method for Measuring Energy Expenditure*; IAEA: Vienna, 1990.
(17) Epstein, S.; Mayada, T. K. *Geochim. Cosmochim. Acta* **1953**, *4*, 213−224.
(18) Brand, W. A.; Avak, H.; Seedorf, R.; Hofmann, D.; Conradi, Th. *Isotopes Environ. Health Stud.* **1996**, *32*, 263−273.
(19) Horita, J.; Ueda, A.; Mitzukami, K.; Takatori, I. *Appl. Radiat. Isot.* **1989**, *40*, 801−805.
(20) Meijer, H. A. J.; Li, W. J. *Isot. Environ. Health Stud.* **1998**, *34*, 349−369.
(21) Begley, I. S.; Scrimgeour, C. M. *Anal. Chem.* **1997**, *69*, 1530−1535.
(22) Murnick, D. E.; Peer, B. J. *Science* **1994**, *263*, 945−947.
(23) Kindness, A.; Marr, I. L. *Appl. Spectrosc.* **1997**, *51*, 17−21.
(24) Fusch, Ch.; Spirig, N.; Moeller, H. *Eur. J. Clin. Chem. Clin. Biochem.* **1993**, *31*, 639−644.

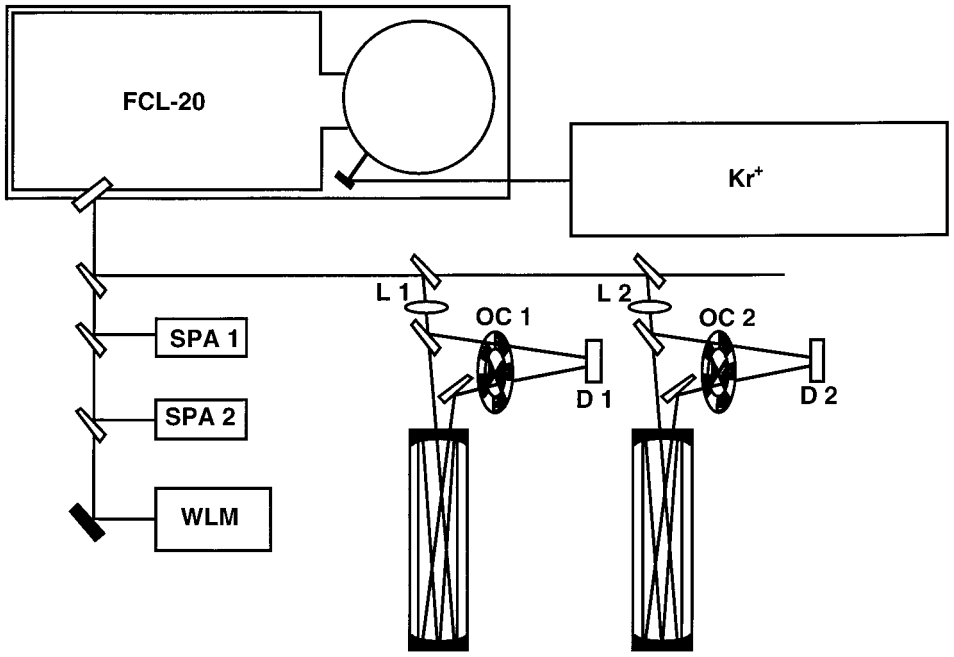

Figure 1. Schematic representation of the experimental setup: FCL-20, color center laser; Kr^+, krypton ion laser; SPA1, 150-MHz FSR spectrum analyzer; SPA2, 8-GHz FSR spectrum analyzer; WLM, wavelength meter; L, 500-mm focal length lens; OC, dual-frequency optical chopper; D, InAs infrared detector.

Table 1. Rovibrational Transitions Used in This Study[a]

frequency (cm^{-1})	intensity[b] ($cm \cdot molecule^{-1}$)	temp coeff[c] at 300 K (K^{-1})	assignment[d]	isotope
3662.920	1.8×10^{-23}	1.3×10^{-3}	$v = (001) \leftarrow (000)$ $J = 5_{15} \leftarrow 5_{14}$	$^1H^{18}O^1H$
3663.045	7.5×10^{-23}	4.4×10^{-3}	$v = (100) \leftarrow (000)$ $J = 6_{24} \leftarrow 7_{17}$	$^1H^{16}O^1H$
3663.321	6.4×10^{-23}	-1.5×10^{-3}	$v = (001) \leftarrow (000)$ $J = 3_{13} \leftarrow 4_{14}$	$^1H^{17}O^1H$
3663.842	1.2×10^{-23}	-3.4×10^{-3}	$v = (001) \leftarrow (000)$ $J = 2_{12} \leftarrow 3_{13}$	$^1H^{16}O^2H$

[a] All values are taken from the HITRAN 1996 spectroscopic database.[30] [b] The intensities are for a natural water sample with abundances: 0.998, 0.00199, 0.00038, and 0.0003 for $^1H^{16}O^1H$, $^1H^{18}O^1H$, $^1H^{17}O^1H$, and $^1H^{16}O^2H$, respectively. [c] The temperature coefficients give the relative change with temperature in absorption intensity of the selected transitions. They are calculated using the HITRAN 1996 database. [d] The notation for the vibrational bands is (ν_1,ν_2,ν_3), whereas the rotational levels are identified by the three quantum numbers J_{KaKc}.

operating for over 2000 h, since a tube refill took place two years ago. The FCL and the other optical components require only occasional readjustments, in practice only after deliberate changes to the optical layout are made.

Two spectrum analyzers and a wavelength meter continuously monitor the FCL output. Only a fraction of the output (~1 mW) is used to record direct absorption spectra in two identical gas cells, equipped with multiple-pass reflection optics. The total optical path length inside the cells is ~20 m. Absorptions outside the cells (due to water and carbon dioxide in the laboratory air) are corrected for by dividing the gas cell signals by the simultaneously recorded laser intensities before the gas cells. For each gas cell, the signal and laser-power beams are amplitude modulated at different frequencies and directed at the same InAs infrared detector. Signal recovery is by means of phase-sensitive detection. In this way, any drift in the operating characteristics of the detector automatically cancels out. A personal computer controls the laser tuning and data acquisition. With a step size of ~15 MHz (0.0005 cm^{-1}) a complete scan over the four selected rovibrational transitions of Table 1 counts ~2000 data points and requires ~2 min.

The gas cells with a volume of ~1 L are filled with 10-μL water samples, using a 10-μL syringe to inject the sample through a silicon membrane ("septum"), resulting in a gas cell pressure of ~13 mbar (the saturated vapor pressure is ~32 mbar). Therewith the signal attenuation is between 25 and 90% for each of the selected transitions and the range of water samples used in this study. This part of the spectrum has been chosen for the fact that all four major isotopic species are present in a small wavelength range and absorb with comparable intensity. The lines are pressure broadened to ~0.008 cm^{-1} (hwhm).

One of the gas cells is filled with reference water with a well-known isotopic composition with respect to the internationally accepted calibration material Vienna Standard Mean Ocean Water (VSMOW). The isotopic composition of the sample water in the second gas cell is determined by comparing the relative intensities of the selected rovibrational transitions in the sample cell to those in the reference cell.

It is customary to express the isotopic composition of a sample with respect to the isotope abundance ratio of a reference (standard) in terms of the δ-value:

$$\delta(x) = \frac{R_x^{\text{sample}}}{R_x^{\text{ref}}} - 1 = \frac{(n_x/n_a)^{\text{sample}}}{(n_x/n_a)^{\text{ref}}} - 1 \qquad (1)$$

The subscript x refers to one of the rare isotopic species (x = $^1H^{18}O^1H$, $^1H^{17}O^1H$, $^1H^{16}O^2H$), while a represents the abundant isotopic species, $^1H^{16}O^1H$. The number density n_z of species z (x, a) is proportional to the absorption coefficient α of the sample at the center frequency ν_z of the corresponding absorption, as given by the Lambert−Beer law: [25]

$$\alpha_z \equiv -\ln(I(\nu_z)/I_0) = S_z\, f(0) n_z\, l \qquad (2)$$

Here, $I(\nu_z)/I_0$ is the ratio of transmitted to incoming laser power at the center of the absorption line. S_z is the line strength of the absorption feature in question, $f(0)$ represents the value of the normalized line shape function evaluated at $\nu = \nu_z$, and l is the absorption path length. In general, $f(0)$ is inversely proportional to the line width. For a Doppler-broadened line with a hwhm of Γ_D: $f(0) = (\ln(2)/\pi)^{1/2}/\Gamma_D$.[25] Thus $n_z \propto \alpha_z\Gamma/(lS_z)$. Since our water samples inside the gas cells are in thermal and pressure equilibrium, the line width Γ is the same for all rovibrational lines in one gas cell, as is the optical path length l. In the superratio of eq 1 the line widths and path length therefore cancel out. Provided the temperature is kept constant and the same for both gas cells, the line strength S will also cancel, and one can replace the number densities in eq 1 with the absorption coefficients of eq 2:

$$\delta(x) = \frac{(\alpha_x/\alpha_a)^{\text{sample}}}{(\alpha_x/\alpha_a)^{\text{ref}}} - 1 = \frac{(\alpha_x^{\text{sample}}/\alpha_x^{\text{ref}})}{(\alpha_a^{\text{sample}}/\alpha_a^{\text{ref}})} - 1 =: \frac{\varphi_x}{\varphi_a} - 1 \qquad (3)$$

The ratio $\varphi_z = (\alpha^{\text{sample}}/\alpha^{\text{ref}})_z$ has been defined here for future use (see eqs 4 and 5). Although in general the line strength S is temperature dependent (predominantly through the ground-state population distribution function), the temperature coefficients of the transitions used in this study are sufficiently small that no special precautions, such as active stabilization of the gas cell temperature, have to be taken in order to avoid measurable temperature effects on the δ-value. Which is not too surprising if one realizes that the δ-value is only sensitive to a temperature difference between the two gas cells.

The line ratios φ are calculated from the experimental data as one of the free parameters in a least-squares approximation of the form

$$-\ln\left(\frac{S_{\text{sample}}(\nu)}{P_{\text{sample}}(\nu)}\right) \cong -\varphi \ln\left(\frac{S_{\text{ref}}(\nu)}{P_{\text{ref}}(\nu)}\right) + \beta_0 + \beta_1(\nu - \nu_z) + \beta_2(\nu - \nu_z)^2 \qquad (4)$$

(25) Demtröder, W. *Laser Spectroscopy, Basic Concepts and Instrumentation*; Springer-Verlag: Berlin, 1981.

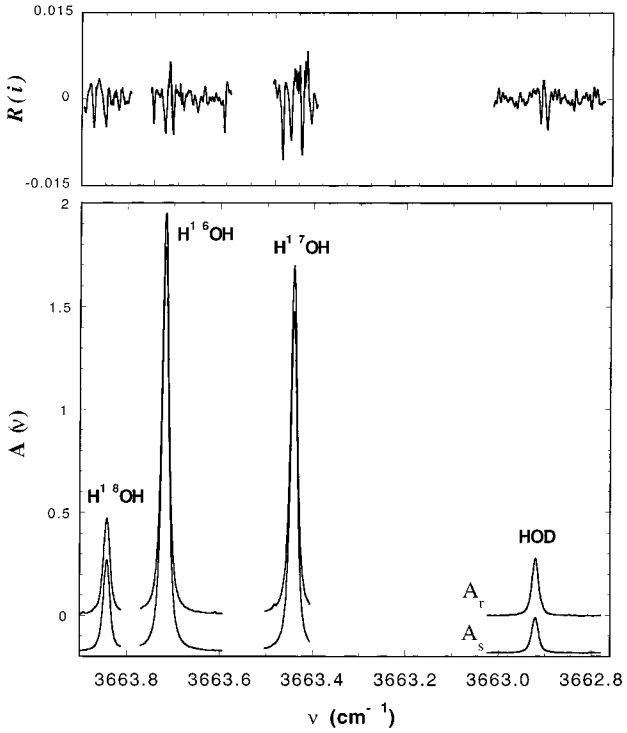

Figure 2. Sample and reference spectra $A(\nu) = -\ln[\text{signal}(\nu)/\text{power}(\nu)]$, together with the residuals $R(\nu)$ as determined by a least-squares approximation according to eq 4. For the reference spectrum A_r the gas cell was filled with the local standard GS-23. The sample cell was filled with a SLAP sample.

Here S and P represent the gas cell absorption spectra and its accompanying power spectrum, recorded for both the sample and reference gas cells as a function of the laser frequency. The three parameters β_k (k = 0, 1, 2) allow for a quadratic "baseline" correction. The fit of eq 4 is carried out for each selected spectral feature (i.e., isotopic species) in a predefined region around the line center at ν_z (see Figure 2). The extent of this spectral section is chosen on a line-by-line basis and reflects the competing requirements of including as much as possible of the baseline and the reduction of spectral overlap with neighboring lines.

The isotope ratio is now determined by

$$\delta(x) = (\varphi_x/\varphi_a) - 1 \qquad (5)$$

As before, x refers to the isotopic species in question (x = $^1H^{18}O^1H$, $^1H^{17}O^1H$, $^1H^{16}O^2H$), while a represents the abundant isotopic species, $^1H^{16}O^1H$. Strictly speaking, the conversion of these *molecular* δ-values to the more common *atomic* δ-values is not straightforward. Fortunately, however, principally due to the fact that the isotope abundance ratios are so small, the two are indistinguishable for all practical applications. Thus, $\delta(^1H^{18}O^1H) = \delta^{18}O$, $\delta(^1H^{17}O^1H) = \delta^{17}O$, and $\delta(^1H^{16}O^2H) = \delta^2H$.

The so-determined δ-values turn out to be rather sensitive to pressure differences between the sample and reference gas cells. Such pressure differences occur in practice due to our inability to inject the ~10-μL water samples with an uncertainty better than ~0.2 μL. The effect is that the line widths in the sample and reference spectra can be measurably different. Since the δ-values

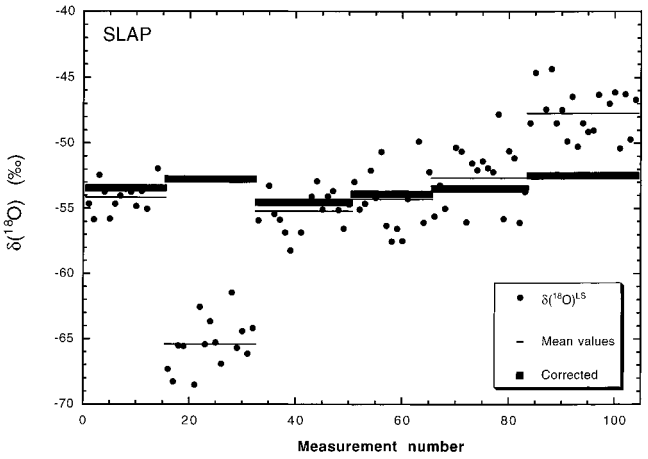

Figure 3. Differential pressure correction using the experimental (average) line width in both the reference and sample spectra as a measure of the pressure differential. The maximum observed relative line width difference amounts to 52‰, corresponding to a δ^{18}O correction term of 12.4‰ or a pressure differential of ~1.2 mbar (for the second measurement series, 16−32).

are determined as a "super" ratio of line intensities, such a line width effect ought to cancel in the final result. That it apparently does not do so is attributed to the particular manner in which the δ-values are determined. Because the rovibrational lines, and in particular the $H^{18}OH$ and $H^{17}OH$ lines of Table 1, show spectral overlap with neighboring lines, the fits of eq 4 are necessarily restricted to a limited spectral range. Consequently, if the line width changes, a different relative portion of the line shape is used in the fit procedure, which has now become sensitive to a differential pressure between the two gas cells. To quantify this effect we have injected water amounts between 8 and 12 μL in the sample cell, while keeping the quantity of the water in the reference cell fixed at 10 μL (with exactly the same isotopic composition). The observed apparent shifts in δ-values suggests a correction to the measured value, δ^*, of the form

$$\delta = \delta^* + \gamma(\Gamma_{\text{sample}} - \Gamma_{\text{ref}})/\Gamma_{\text{ref}} \qquad (6)$$

The gas cell pressure differential is thus determined by measuring the relative difference in the (average) line widths in the sample and reference spectra. The value of γ was determined experimentally to be $\gamma(^1H^{18}O^1H) = -0.248(16)$, $\gamma(^1H^{17}O^1H) = -0.330(8)$, and $\gamma(^1H^{16}O^2H) = 0.016(17)$. The relative sizes of these correction parameters reflect the importance of spectral overlap in the determination of the respective δ-values. Results of a normal measurement for $\delta(^1H^{18}O^1H)$ are shown in Figure 3. It may be clear that the correction of eq 6 is significant in this case, corresponding to a deviation of ~10 per mil points per mbar pressure change (‰/mbar).

A typical measurement series ("run") consists of ~15 individual laser scans over the spectral section encompassing the four rovibrational lines of Table 1. For each individual scan, the δ-values are calculated for all three isotopic species according to the above-described fitting procedure. After the correction of eq 6 is applied, accidental outliers (all values removed from the median by more than twice the absolute deviation) are removed (usually no more than 2 out of 15). The average value of the remaining measurements is reported as the final result, together with its standard error. Including sample introduction and gas cell evacuation between the measurement series, one run takes a little less than 1 h.

An in-depth treatment of the experimental setup, including a numerical investigation of the data analysis procedure, will be presented elsewhere.[26]

CALIBRATION

To calibrate the instrument we measured the (IAEA) reference material GISP (Greenland Ice Sheet Precipitation), as well as a series of local water standards that are well-characterized with respect to VSMOW by repeated mass spectrometer analyses in our laboratory (see Table 4). The local standard GS-23 was used as working standard in the reference gas cell. Consequently, the laser spectrometer (LS) values are initially referenced to this material. These have been converted to values relative to VSMOW, using the laser spectrometrically determined value of GS-23 with respect to VSMOW. This inherently takes care of the zero-point adjustment of the laser spectrometric δ-scale.

In Figure 4 we present the resulting calibration curves for the three isotopic species. In the case of $^1H^{17}O^1H$, the GS-32 local standard was excluded from the test. For all other water samples, the ^{17}O isotope ratio is known through its relation with the ^{18}O isotope ratio:[20]

$$1 + \delta(^{17}O) = [1 + \delta(^{18}O)]^{0.5281} \qquad (7)$$

As the ^{2}H, and to a lesser extend the O, measurements are afflicted with a large memory effect (the influence of the previous sample on the current measurement), it turned out to be occasionally necessary to inject three or more water samples before the measured δ-value reached its final value. To minimize the influence of this memory effect on the calibration procedure, large steps in δ-values between subsequent samples were avoided as much as possible. For the same reason, Figure 4 includes data recorded both in increasing and in decreasing order of δ-value. In the future, the gas cells may be operated at an elevated temperature in order to promote a quicker water removal from the cells.

The calibration data of Figure 4 are fit to linear functions with variable slope. The rms value of the residuals gives a good indication of the overall accuracy of the method, including all effects of sample handling. The values are 2.8, 0.7, and 1.3‰ for δ^2H, δ^{17}O, and δ^{18}O, respectively. The precision of the method is given by the standard error of the individual results of one series of (typically) 15 laser scans. The current average values of these are 0.7, 0.3, and 0.5‰ for δ^2H, δ^{17}O, and δ^{18}O, respectively. In the case of ^{17}O and ^{18}O, the precision can still be improved by increasing the number of laser scans in one run (i.e., increasing the measuring time). For $\delta(^2H)$ the minimum standard error has already been reached at this point, indicating that the precision in this case is limited by sample-handling errors, including memory effects and isotope fractionation at the gas cell walls. In fact, extensive fractionation at the walls is to be expected, in particular for hydrogen. However, such fractionation is only

(26) Kerstel, E. R. Th.; van Trigt, R.; Meijer, H. A. J., in preparation.

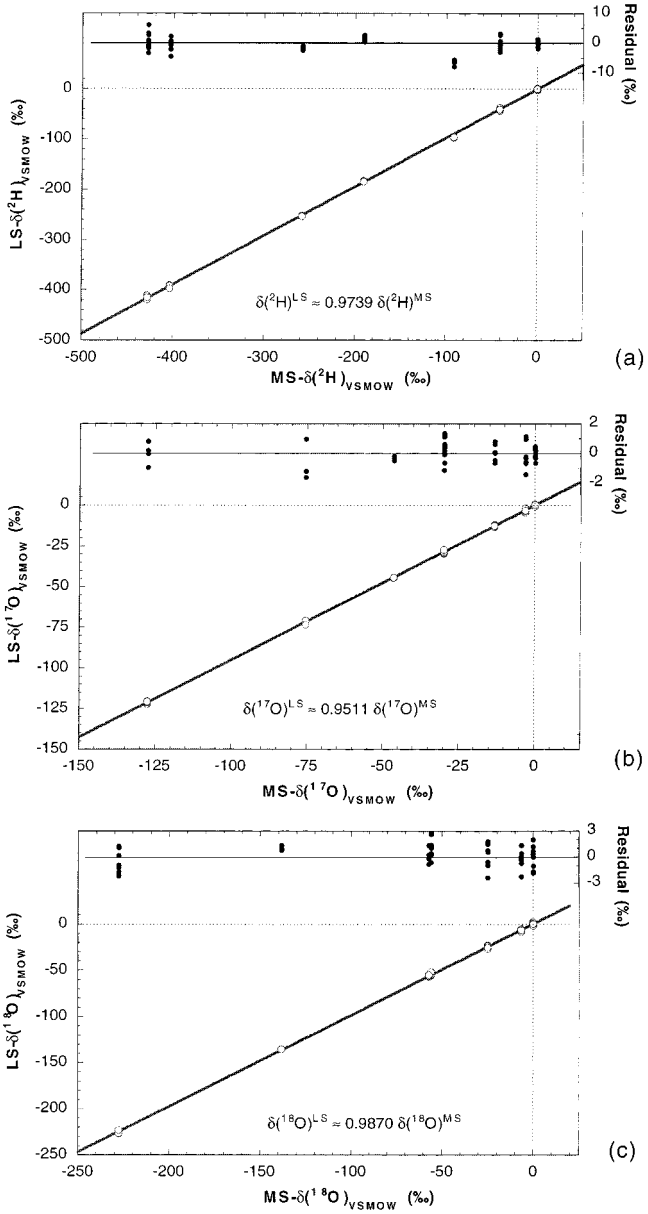

Figure 4. Calibration curves for (a) δ^2H, (b) δ^{17}O, and (c) δ^{18}O. The root-mean-square deviations of the residuals are 2.8, 0.7, and 1.3‰, respectively.

Table 2. Slap δ-Values (‰) (Referenced to VSMOW)

isotope	laser spectrometer[a]	consensus value[b]
$\delta(^2H)$	−415.47 (0.85)	−428.0
$\delta(^{17}O)$	−28.11 (0.23)	−29.70
$\delta(^{18}O)$	−53.88 (0.37)	−55.5

[a] Based on 11 measurement series (or runs, each consisting of 15 individual laser scans) and acquired over a one-month interval. The standard error is given in parentheses. [b] Consensus value, recommended by the IAEA.[28] The δ^2H value results from a mixture of isotopically pure synthetic waters and is regarded to be correct in absolute terms. The δ^{18}O is the consensus value of 25 laboratories; the true value is likely somewhat more negative.[27] The δ^{17}O value is based on the consensus δ^{18}O value in combination with eq 7.

observable to the extent that the two gas cells behave differently. If such is the case, injecting exactly the same water sample in both cells will result in a δ-value significantly different from zero.

Table 3. Results for VSMOW and SLAP, against VSMOW and Scaled to the SLAP Consensus Values as Reported in Table 2[a]

sample	$\delta(^2H)$	$\delta(^{17}O)$	$\delta(^{18}O)$
VSMOW	1.17 (0.60)	0.49 (0.27)	1.25 (0.66)
VSMOW	−1.63 (0.65)	0.25 (0.24)	2.11 (0.44)
VSMOW	−0.07 (1.05)	−0.22 (0.31)	0.35 (0.70)
VSMOW	0.23 (0.99)	0.29 (0.28)	0.70 (0.73)
VSMOW	−0.09 (0.80)	−0.09 (0.32)	−1.00 (0.33)
VSMOW	−1.41 (0.97)	−0.28 (0.39)	−1.66 (0.46)
VSMOW	1.30 (0.96)	−0.66 (0.19)	−1.82 (0.72)
VSMOW	0.49 (0.83)	0.22 (0.31)	0.07 (0.38
std dev	1.07	0.38	1.40
SLAP	−426.04 (0.47)	−31.23 (0.18)	−56.52 (0.33)
SLAP	−426.21 (0.43)	−30.00 (0.25)	−56.35 (0.38)
SLAP	−422.76 (1.55)	−28.74 (0.28)	−55.35 (0.43)
SLAP	−426.30 (0.39)	−29.52 (0.23)	−55.55 (0.31)
SLAP	−428.77 (0.29)	−29.84 (0.22)	−57.44 (0.52)
SLAP	−429.92 (0.33)	−30.73 (0.32)	−55.73 (0.48)
SLAP	−425.71 (0.80)	−29.39 (0.38)	−53.91 (0.46)
SLAP	−430.83 (1.19)	−28.61 (0.47)	−55.70 (0.82)
SLAP	−430.74 (0.51)	−29.63 (0.55)	−56.50 (0.56)
SLAP	−432.60 (0.39)	−30.12 (0.28	−54.06 (0.54)
SLAP	−428.11 (0.36)	−28.88 (0.38)	−53.38 (0.38)
std dev	2.89	0.81	1.26

[a] Within parentheses the standard errors (all in per mil points), as well as the standard deviation.

This we do not observe. It should be noted that fractionation between the liquid and gas phases of water is avoided by working at a substantially lower pressure (13 mbar) than the saturated vapor pressure (32 mbar at room temperature): all injected liquid water quickly evaporates inside the evacuated gas cell.

The slopes of the calibration curves are all different from unity: laser spectrometry underestimates the isotope ratios. It appears as if the sample is mixed with reference water (but not vice versa, as cross-contamination would lead to a quadratic deviation,[27] which is not observed). Although we have established that the sample introduction procedure cannot be blamed, we have not yet been able to eliminate this residual effect (perhaps caused by memory effects in the vacuum system).

As has become apparent over the years in numerous international ring tests, IRMS-based measurements too exhibit calibration curves with slopes smaller than unity, and in particular, for ^{2}H the deviations found are often much larger than those of the present laser system. A pragmatic approach to these problems, in which the δ-scales are defined by a linear calibration using two different calibration waters (e.g., SLAP in addition to VSMOW), has been generally accepted and, in fact, is recommended by the IAEA.[28,29] The same solution can be applied to our laser-based method, even more so, since the reproducibility of the measurements is rather good, especially considering that the results of

(27) Meijer, H. A. J.; Neubert, R., submitted to *Int. J. Mass Spectrom.*
(28) Gonfiantini, R. *Advisory Group Meeting on Stable Isotope Reference Samples for Geochemical and Hydrological Investigations;* IAEA: Vienna, 1984.
(29) Hut, G. *Consultants' Group Meeting on Stable Isotope Reference Samples for Geochemical and Hydrological Investigations;* IAEA: Vienna, 1986.
(30) Rothman, L. S.; Rinsland, C. P.; Goldman, A.; Massie, S. T.; Edwards, D. P.; Flaud, J.-M.; Perrin, A.; Camy-Peyret, C.; Dana, V.; Mandin, J.-Y.; Schroeder, J.; McCann, A.; Gamache, R. R.; Wattson, R. B.; Yoshino, K.; Chance, K. V.; Jucks, K. W.; Brown, L. R.; Nemtchinov, V.; Varanasi, P. *J. Quant. Spectrosc. Rad. Trans.* **1998**, *60*, 665−710.

Table 4. Laser Spectrometry Compared to Mass Spectrometry[a]

	mass spectrometry			laser spectrometry			
standard[b]	$\delta(^2H)$	$\delta(^{17}O)$[c]	$\delta(^{18}O)$	$\delta(^2H)$	$\delta(^{17}O)$	$\delta(^{18}O)$	N
VSMOW	0.0	0.0	0.0	0.0 (0.4)	0.0 (0.13)	0.0 (0.5)	8
SLAP	−428.0	−29.70	−55.5	−428.0 (0.9)	−29.7 (0.2)	−55.5 (0.4)	11
GISP	−190.0	−13.21	−24.76	−188.8 (0.3)	−13.2 (0.3)	−25.0 (0.5)	8
GS-23	−41.0	−3.36	−6.29	−41.4 (0.8)	−3.3 (0.3)	−6.7 (0.4)	8
GS-31	−257.8	−75.48	−137.3	−260.5 (0.4)	−76.5 (0.9)	−139.3 (0.2)	3
GS-30	−403.3	−127.55	−227.7	−405.4 (0.8)	−128.0 (0.4)	−232.5 (0.5)	8
GS-32	−91.5		−56.84	−98.6 (0.5)	−46.9 (0.10)	−58.0 (0.5)	4

[a] The LS results are based on between $N = 4$ and 11 δ-determinations (of 15 individual laser scans each), spread out in time over a period of between 4 and 10 weeks. all values are expressed in per mil points. the standard error of the mean values reported for the LS measurements is given in parentheses. [b] The VSMOW and SLAP values for δ^2H and $\delta^{18}O$ are those recommended by the IAEA.[28] The reference material GISP has the consensus values (ref 28): $\delta^2H = -189.7$ (1.1)‰ and $\delta^{18}O = -24.79$ (0.09)‰. The Groningen GS local standards have been established by repeated mass spectrometric analysis in our laboratory over a period of several years. GS-23 is a natural water; GS-30, GS-31, and GS-32 are synthesized. [c] The $\delta^{17}O$ values of those water samples that exhibit a natural relation between the ^{17}O and ^{18}O abundance ratios (i.e., all except GS-32) have been calculated from $(1 + \delta^{17}O) = (1 + \delta^{18}O)^{\lambda}$, with $\lambda = 0.5281$ (0.0015) (see ref 20).

Figure 4 were gathered over an extended period of time (about two months). This means that the system is now ready to be applied to the biomedical doubly labeled water method to measure energy expenditure, as well as to the accurate measurement of natural abundances, for which especially the δ^2H determination is already competitive.

The VSMOW−SLAP linear calibration and its results are summarized in Tables 2−4. In Table 2, the mean of the LS δ-values (referenced to VSMOW), which determined the scale expansion factor, is compared with the respective IAEA consensus values for each of the isotopes. In Table 3, the individual measurements for VSMOW and SLAP are presented, again referenced to VSMOW and this time after linear calibration (i.e., the mean of these measurements equals the corresponding IAEA consensus value). Finally, Table 4 confronts the LS results with the MS results by comparing the current "best" values for a series of seven water samples (including VSMOW and SLAP, which define the linear calibration).

CONCLUSIONS

We have shown that laser spectrometry presents a promising alternative to conventional mass spectrometric isotope ratio analysis of water. In particular, the laser-based method is conceptually very simple and does not require cumbersome, time-consuming pretreatments of the sample before measurement. This excludes an important source of errors. Moreover, all three isotope ratios, $^2H/^1H$, $^{18}O/^{16}O$, and $^{17}O/^{16}O$ (virtually impossible by means of IRMS), are determined at the same time without requiring different (chemical) pretreatments of the sample.

The precision of the method is currently ∼0.7‰ for $^2H/^1H$ and 0.5‰ for the oxygen isotopes. We have shown a calibrated accuracy of about 3‰, respectively, 1‰. Since the calibration data were collected over an extended period in time, it is expected that more frequent calibration will enable us to achieve an accuracy closer to the intrinsic precision of the apparatus. In addition, the calibration procedure will be improved by the simultaneous measurement of more than one standard water (i.e., for natural abundance measurements one would use two local laboratory standards, one close to VSMOW in isotopic composition, the other close to SLAP). In particular, the standards should be chosen each at one end of the expected range of δ-values, not near to one end as is the case here for $\delta(^{17}O)$ and $\delta(^{18}O)$.

Currently, the throughput is limited to about one sample per hour, comparable to that of the original, conventional methods when both δ^2H and $\delta^{18}O$ are determined and the sample preparation time is added to the actual IRMS time. With modest improvements in the detection (faster amplitude modulation and a shorter lock-in time constant), this can probably be increased by a factor of 2, the final limiting factor being the evacuation and flushing of the gas cells. However, the throughput is most easily increased by the use of multiple gas cells, allowing the parallel measurement on many more than just one sample. Considering the very modest demands on laser power, relative to the output power of the available laser system, the number of gas cells is only limited by budgetary and space constraints.

ACKNOWLEDGMENT

We thank Jaap van der Ploeg for his excellent technical support and Prof. Sigfus Johnsen and Prof. Wim Mook for their continued interest in our work. We are grateful to the Stichting FOM and the Groningen Isotech Foundation for providing financial support. E.R.Th.K. thanks the Royal Dutch Academy of Sciences (KNAW) for a young investigator fellowship.

Received for review June 10, 1999. Accepted September 7, 1999.

AC990621E